Dynamics of an oscillating wave surge converter: an analysis on the influence of the bottom slope

DOI: 10.46932/sfjdv4n1-024

Received in: January 30th, 2023
Accepted in: February 28th, 2023

Guilherme Fuhrmeister Vargas
PhD in Water Resources
Institution: Universidade Federal do Rio Grande do Sul (UFRGS) - Instituto de Pesquisas Hidráulicas
Address: Av. Bento Gonçalves, 9500, prédio 44302, Agronomia, Porto Alegre - RS, Brasil
E-mail: guilhermef.engenharia@gmail.com

Edith Beatriz Camaño Schettini
PhD in Fluid Mechanics and Transport Phenomena
Institution: Universidade Federal do Rio Grande do Sul (UFRGS) - Instituto de Pesquisas Hidráulicas
Address: Av. Bento Gonçalves, 9500, prédio 44302, Agronomia, Porto Alegre - RS, Brasil
E-mail: bcamano@iph.ufrgs.br

Bruno Alavarez Scapin
Master in Water Resources
Institution: Universidade Federal do Rio Grande do Sul (UFRGS) - Instituto de Pesquisas Hidráulicas
Address: Av. Bento Gonçalves, 9500, prédio 44302, Agronomia, Porto Alegre - RS, Brasil
E-mail: bruno.scapin@hotmail.com

ABSTRACT
The Oscillating Wave Surge Converter represents a technology with great potential for generating electricity from ocean waves, promoting energy continuously throughout a day. Its development is on a pre-commercial scale and has been encouraging several companies and institutions to invest in the improvement and study of this conversion system. Simulations in Computational Fluid Dynamics are very important tools for the development of these converters, since they provide essential details for the analysis of the variables that influence the system. In this context, the present work uses the Large Eddy Simulation modeling to study the influence of the bottom slope on the device dynamics, which is performed using the OpenFOAM v.4.1 computational code and its extension OlaFlow. The model used in the analysis is two-dimensional and based on the Wall-Adapting Local Eddy-Viscosity methodology, while a structured mesh is applied. Through a detailed analysis, it was observed that the converter hydrodynamics is strongly influenced by the bottom slope, which is responsible for the intensification of the captured power in regions with slopes lower than 5º, and for the power decrease in cases where the slope exceeds 15º. Significant increases in slope can cause a decrease up to 28% in the converter excitation torque, significantly affecting its performance in electric power generation.

Keywords: wave energy converter, *oscillating wave surge converters*, openfoam, olaflow, large eddy simulation.

1 INTRODUCTION

The current global scenario is characterized by a society aware that the release of carbon dioxide, hydrocarbons and several other chemical components into the atmosphere is highly harmful, causing significant variations in the temperature and the climate of the planet. Therefore, several organizations, companies and researchers invest and encourage the use of alternative energy technologies. Among these, is the energy from sea waves, which have a worldwide potential of 2 TW and are capable of generating electricity over 24 hours a day. This renewable energy can also be associated with other renewable sources, such as wind and solar (Jin, Zheng, Greaves, 2022).

In this scenario, new systems capable of converting wave energy have been studied and developed, while other renewable systems are constantly being improved (Curto, Franzitta, Guercio, 2021). Some of the converters are on a pre-commercial scale of development, such as the Oscillating Wave Surge Converters – OWSC's (Ghasemipour, Izanlou, Jahangir, 2022). This system represents one of the greatest potentials for the electric energy production, as demonstrated on the work presented by Kelly et al. (2021).

The operating system of an OWSC (Figure 1) consists on capturing the horizontal component of the waves, which is responsible for causing the oscillatory movement of a floating flap back and forth, driving a hydraulic piston, which powering a turbine for generating electricity (Gallutia et al., 2022). These structures can be installed completely submerged (Figure 2a) or partially submerged on floating platforms (Figure 2b), which represents a flexibility of the system, allowing the OWSC's to be located in different regions of the ocean.

Figure 1.- Working principle of an Oscillating Wave Surge Converter

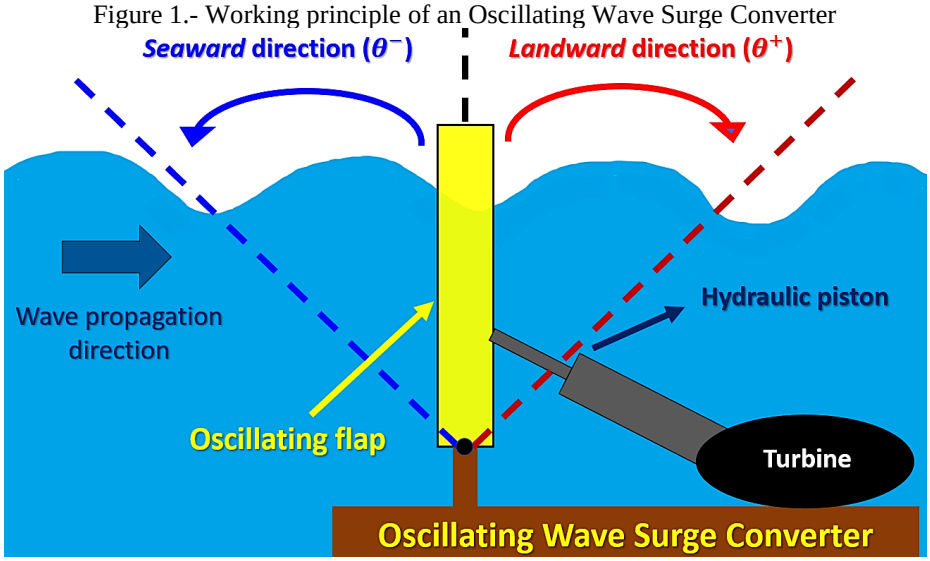

Nowadays, computational numerical simulations in fluid mechanics (Computational Fluid Dynamics - CFD) represent one of the main tools used in the projects and studies of these and several other energy conversion systems, allowing the analysis of different installation configurations,

geometries, wave characteristics, and flow conditions (Windt, Davidson, Ringwood, 2018). In addition, numerical modeling allows for obtaining very detailed data about velocity fields, pressure gradients, and experienced forces, thus being fundamental to experimental studies, usually performed in laboratories (Esteban et al., 2022).

Figure 2.- Different configurations of an OWSC: a – fully submerged, b – partially submerged (National Renewable Energy Laboratory, 2021; Langlee Wave Power, 2013).

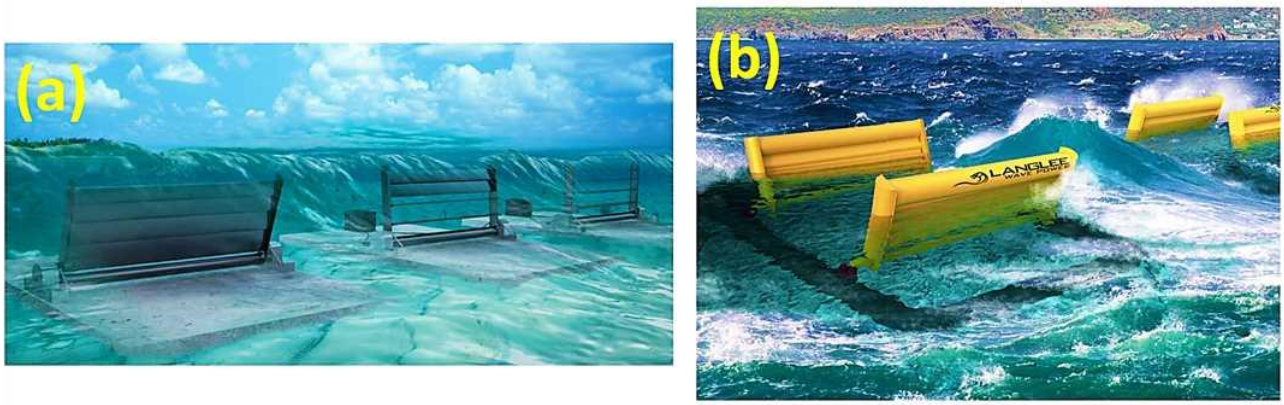

Several relevant numerical works have been published over the last few years, allowing the analysis and the study of the complex flow conditions involved in the device hydrodynamics. Among these are the works by Liu et al. (2022), Liu, Wang, and Hua (2021), Brito et al. (2020), Wei et al. (2016), and Wei et al. (2015), which represent important references in the area and demonstrate the significant role of numerical simulations in the analysis of OWSC's. However, CFD studies generally use the Reynolds Averaged Navier-Stokes (RANS), Smoothed Particle Hydrodynamics (SPH), and Potential Flow methods, which often fail to capture the significant fluctuations related to the flow fields due to turbulence. On the other hand, the Large Eddy Simulation (LES) method represents a powerful tool for the numerical analysis of several cases in ocean engineering, even if it does not yet have many expressive applications in this area (Bourgoin et al., 2020).

Considering the limited application of LES modeling in the study of wave energy converters, added to the fact that the influence of the bottom slope on the hydrodynamics of the OWSC is still unknown, the main objective of this work is to complete these two existing gaps.

2 NUMERICAL METHODOLOGY

This study is performed using the free and open-source computational code OpenFOAM v.4.1, combined with its OlaFlow extension, which is based on the Finite Volume Methodology and the Volume of Fluid method (VOF) for the free surface representation (Higuera 2016). This numerical code is powered by a complex mathematical library and several boundary conditions, allowing the user to adapt them to

the most diverse cases of the flow. Furthermore, the numerical schemes can work with the precision of up to the fourth order, providing realistic and detailed results of the associated phenomena.

Mathematical modeling based on the LES methodology consists of the application and numerical resolution of the continuity and Navier-Stokes equations, which can be written in tensor notation, in sequence, by the following expressions (Launchbury, 2016):

$$\frac{\partial \bar{u}_i}{\partial x_i} = 0\,, \quad [1]$$

$$\frac{\partial \bar{u}_i}{\partial t} + \frac{\partial (\bar{u}_i \bar{u}_j)}{\partial x_j} = \bar{f}_i - \frac{1}{\rho}\frac{\partial \bar{P}}{\partial x_i} + \frac{\partial}{\partial x_j}\left(\nu \left[\frac{\partial \bar{u}_i}{\partial x_j} + \frac{\partial \bar{u}_j}{\partial x_i}\right]\right) - \frac{\partial {\tau_{ij}}^{sgs}}{\partial x_j}\,, \quad [2]$$

where $\bar{u}_{i,j}$ represents the related velocity of large scales, $x_{i,j}$ the position, t the time, $\bar{f}_i$ the term of gravitational forces, ρ the water density, $\bar{P}$ the filtered pressure by the LES method, ν is the kinematic viscosity of the fluid, and ${\tau_{ij}}^{sgs}$ is the stress tensor of the sub-grid scales (solved by the LES-based turbulence model).

The LES model used in the present work is the Wall-Adapting Local Eddy-Viscosity (WALE), in which the large scales are filtered according to the volumes of the numerical mesh elements, making it possible to model the regions close to the solid contours and the regions of flow transition. For this reason, this model is quite suitable for the present study. Its numerical validation was performed based on an extreme situation of operation of the OWSC's (known as Slamming), described by Wei et al. (2016), which is presented in detail in the work of Fuhrmeister (2020).

2.1 ADAPTATION OF MESH ELEMENTS OVER TIME

For the representation of rigid body dynamics as a function of wave dynamics, the methodology known as the mesh morphing method was used, which consists of deforming the mesh elements over time, preserving the topology of the solid object. The solver of the OpenFOAM code based on this method is known as dynamicMotionSolverFvMesh, while the displacementSBRStress solver is responsible for adjusting the elements to the domain.

2.2 NUMERICAL DOMAIN AND FLAP DIMENSIONS

The numerical domain of the present study corresponds to a box 8,40 m wide, 3,80 m high and 0,80 m deep (Figure 3). It is composed of an inlet, an outlet, a top, a bottom and two sides (inside and outside the page), the latter being taken as empty values (as a result of the model being two-dimensional).

The flap applied in the simulations is 0,40 m high, 0,08 m thick, 0,80 m wide (equal to the domain width, which is typical of two-dimensional simulations) and has a density of 219,00 kg/m³. Its centroid is located exactly at the geometric center of the box, whose axis of rotation (intowards the page) is located on the centerline of the lower base of the structure. The flap is 4,20 m from the inlet, and its lower base is at a distance of 0.12 m from the bottom.

Given the goal of this work, a small ramp with slope β and height h_t was used, with the values changing in all simulations to correspond to the various case studies (for this reason, the water level h is modified in each analysis). To avoid wave breaking over the flap and the effects of wave reflection, the flat part of the ramp was designed so that there is always a column of water in the region close to the outlet.

Figure 3.- Numerical domain and geometric characteristics of the OWSC used in the simulations.

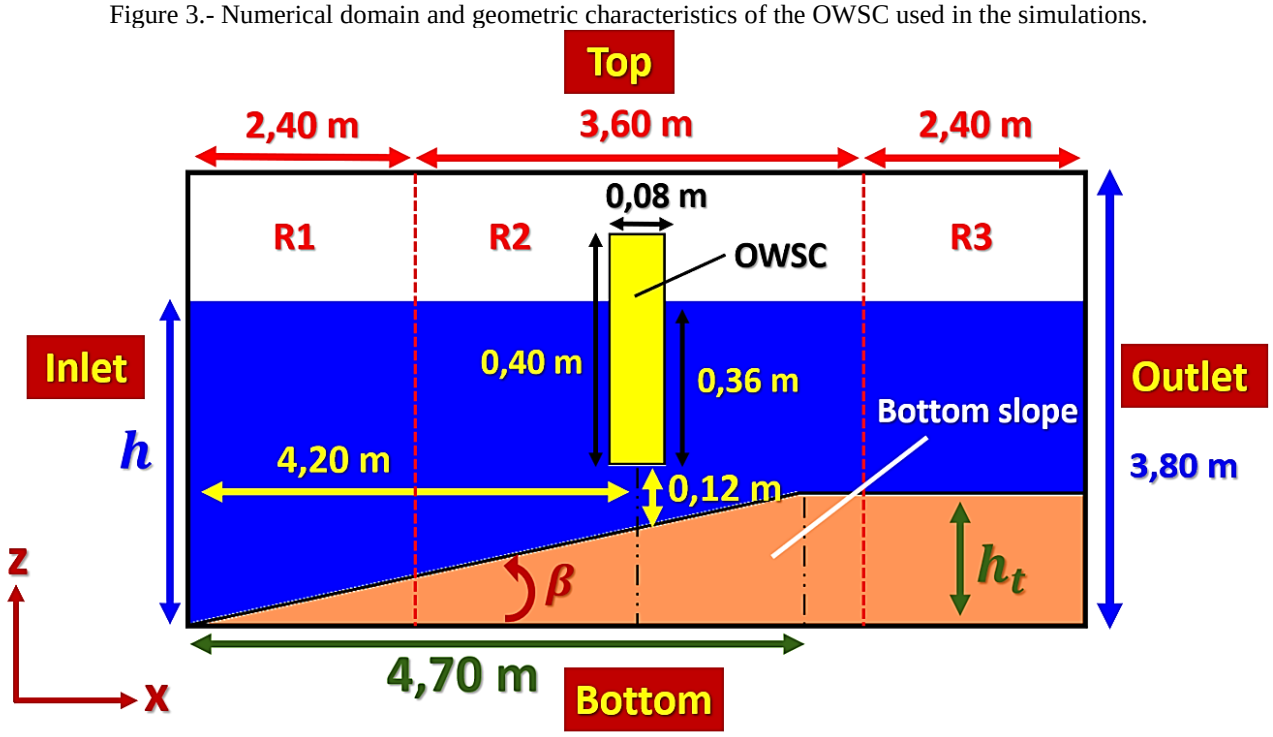

2.3 CHARACTERISTICS OF THE NUMERICAL MESH

The numerical mesh applied is uniform and structured, composed of hexahedral elements, which facilitates the representation of the free surface and its mathematical formulation. There are three regions on the grid (R1, R2, and R3), with the central region having the highest level of mesh refinement. The mesh discretization characteristics were defined as follows:

$$\Delta x_{R2} = \Delta z_{R1} = \Delta z_{R2} = \Delta z_{R3} = 0{,}01\ m\ , \qquad [3]$$

$$\Delta x_{R1} = \Delta x_{R3} = 5.\Delta x_{R2}\,. \qquad [4]$$

2.4 INITIAL AND BOUNDARY CONDITIONS

At the inlet, the outlet, and the top of the domain, the conditions for generating regular waves (of defined height and period), a sponge layer (to absorb the effects of the incident wave), and outflow were applied, respectively. At the bottom of the domain, the non-slip condition was used, while at the flap, the moving wall condition was applied. In Table 1, all boundary conditions are arranged according to their respective nomenclature in the OpenFOAM code.

While the flap is initially vertical and orthogonal to the bottom and top of the domain, the initial conditions for velocity and pressure are both zero-valued internal fields. The initial time step (Δt) adopted was 0,01 s; however, it is allowed to be readjusted at each step due to the deformation of the numerical mesh elements, optimizing the convergence of the simulations and allowing a Courant number lower than 0,8.

Table 1. – Boundary conditions applied, according to their nomenclature in the OpenFOAM code

Boundary	Velocity condition	Pressure condition
Inlet	*waveVelocity*	*fixedFluxPressure*
Outlet	*waveAbsorption2DVelocity*	*fixedFluxPressure*
Top	*pressureInletOutletVelocity*	*totalPressure*
Bottom	*noSlip*	*fixedFluxPressure*
Bottom ramp	*noSlip*	*fixedFluxPressure*
Flap	*movingWallVelocity*	*fixedFluxPressure*
Sides	*empty*	*empty*

3 RESULTS

The dynamics of a regular incident wave of 0,10 m height (H) and 1,90 s period (T) was considered in all cases analyzed in this work. Likewise, a fixed flap submergence of 90% was also considered (with a submerged depth equal to 0,36 m, as presented in Figure 3).

In order to analyze the influence of the bottom slope on the hydrodynamics of the OWSC, seven different values of β were considered, which result in different values of h_t and h. These cases are described in Table 2.

Tabela 2. – Characteristics of the cases

Case	β (°)	h_t (m)	h (m)
1	0,00	0	0,48
2	4,75	0,39	0,83
3	9,50	0,79	1,18
4	14,24	1,19	1,55
5	19,00	1,62	1,93
6	23,74	2,07	2,33
7	28,49	2,55	2,76

Figure 4 shows the velocity fields for cases 1, 2, 4, and 7, considering the instants of maximum angular displacement in the landward and seaward directions. In this figure, it can be observed that the maximum angular displacement in both directions are quite similar in all cases. However, it is possible to observe an intensification of the velocity magnitudes with the increase of the bottom slope. Similarly, there is also an intensification of vorticity around the lower region of the flap in cases of higher β values. In the latter, where the bottom slope is higher, there is a tendency for recirculation zones to occur underneath the structure.

Figure 4.- Velocity fields for the maximum angular displacement observed in the landward and seaward directions (cases 1, 2, 4 and 7)

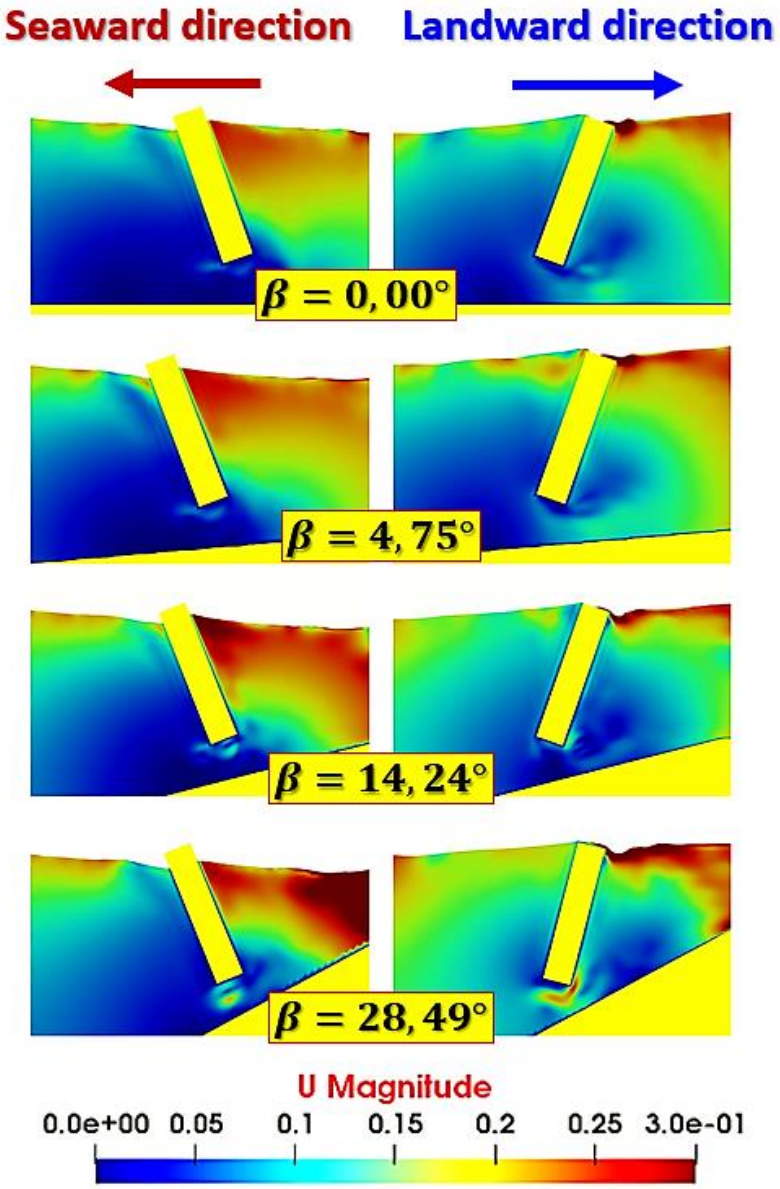

A comparison between the maximum and minimum values observed is performed for angular displacement (θ), angular velocity (ω), horizontal force (F_h), vertical force (F_V) and excitation torque

(M). Such results are represented in the graphs in Figure 5, where the modules of maximum (Max_{Amp^+}, related to θ^+) and minimum (Max_{Amp^-}, related to θ^-) values observed are presented.

According to Figure 5a, it is observed that the highest values of angular displacement occur in the landward direction up to a slope close to 15°, and, for larger values, the highest angular displacement starts to occur in the seaward direction (a fact that can be correlated to the occurrence of recirculation zones below the flap, as observed in the velocity fields of Figure 4). On the other hand, for very small slopes (close to 0°), it is observed that the maximum amplitudes reached in the positive and negative directions are very similar.

The magnitude of the maximum positive angular velocity increases up to a slope close to 15º, tending to stabilize on higher slopes at a value close to 1.80 rad/s (Figure 5b). However, for the same conditions, the magnitude of the maximum negative angular velocity tends to decrease to a value around 1,00 rad/s, stabilizing at values close to this in slopes greater than 15°.

Through the analysis of Figure 5c, it is verified that the module of the maximum values observed for the horizontal force tends to increase for slopes between 0° and 5°. However, for higher values, the magnitudes of both maximum amplitudes are quite similar, close to 50 N, showing that the oscillation of the flap tends to decrease with the increase of the bottom slope. On the other hand, in Figure 5d it is observed that the difference between the maximum amplitudes reached is practically constant, leading to the conclusion that the vertical force does not present significant changes in function of the bottom slope.

For slopes with values lower than 10°, the maximum amplitude observed for the excitation torque in the seaward direction is greater than the amplitude reached in the landward direction (Figure 5e). For slopes greater than 10°, an inversion between the maximum amplitudes is observed, however, the difference between both becomes practically constant, indicating that, in very steep bottoms, the flap tends to rotate with greater intensity towards the landward direction.

Figura 5.- Magnitudes of maximum positive amplitudes (or landward direction) and maximum negative amplitudes (or seaward direction) as a function of the bottom slope, considering angular displacement (a), angular velocity (b), horizontal force (c) , vertical force (d) and the excitation torque (e).

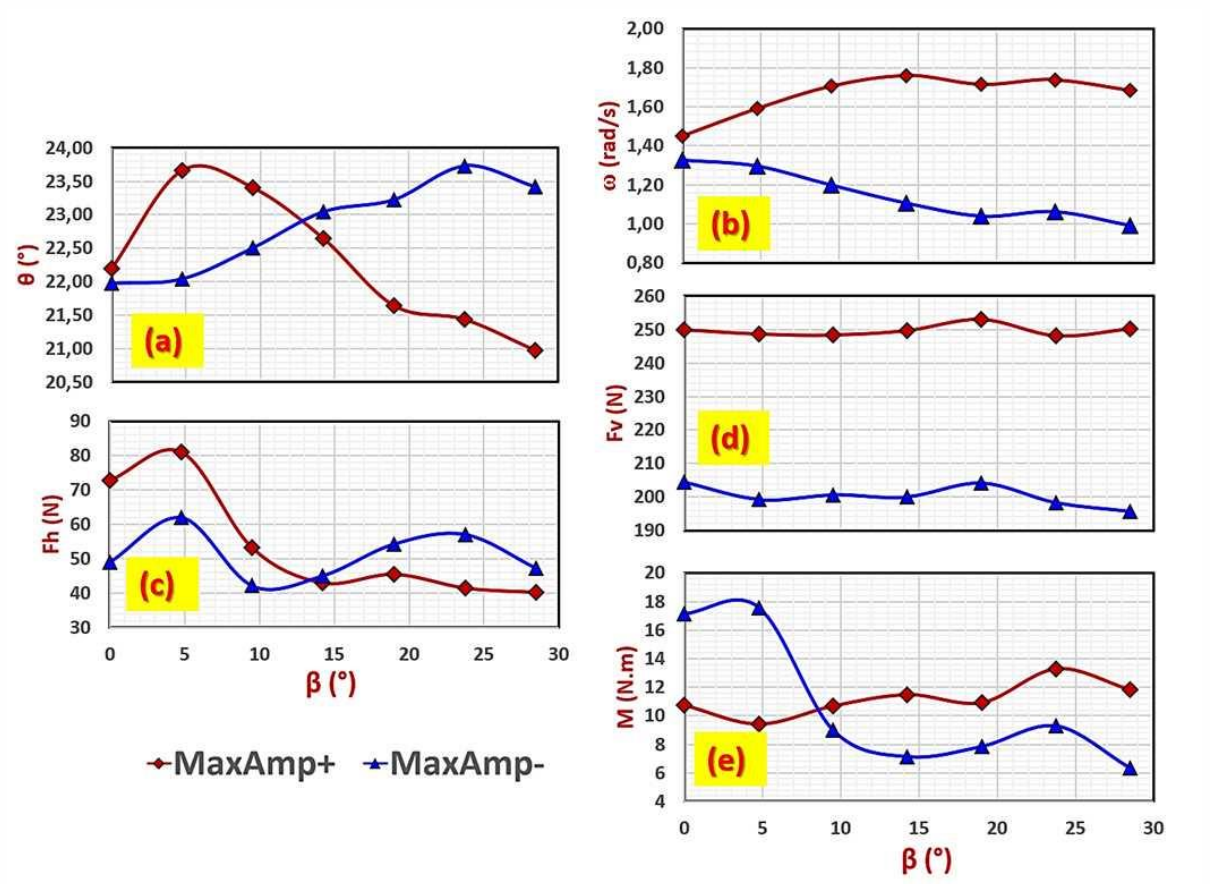

Considering the objective of studying the hydrodynamic influences on the OWSC as a function of the bottom slope, the root mean square values (RMS) of the same variables previously analyzed were evaluated, whose results are shown in the graphs of Figures 6 and 7. An estimate of the average captured power (Pot_{Med}) can be obtained by multiplying the RMS values of the angular velocity and the excitation torque (Figure 7b):

$$Pot_{Med} \approx \omega_{RMS}.M_{RMS} . \qquad [5]$$

As shown in Figure 6a, the angular displacement first tends to increase for a slope of up to 5° (increase of approximately 3,20%), starting to decrease for slopes greater than this value (representing a decrease of up to 16%, when compared to the maximum value observed for the angular displacement).

Figure 6.- Variation of the RMS value of the angular displacement, angular velocity, horizontal force and vertical force experienced by the OWSC, as a function of the bottom slope.

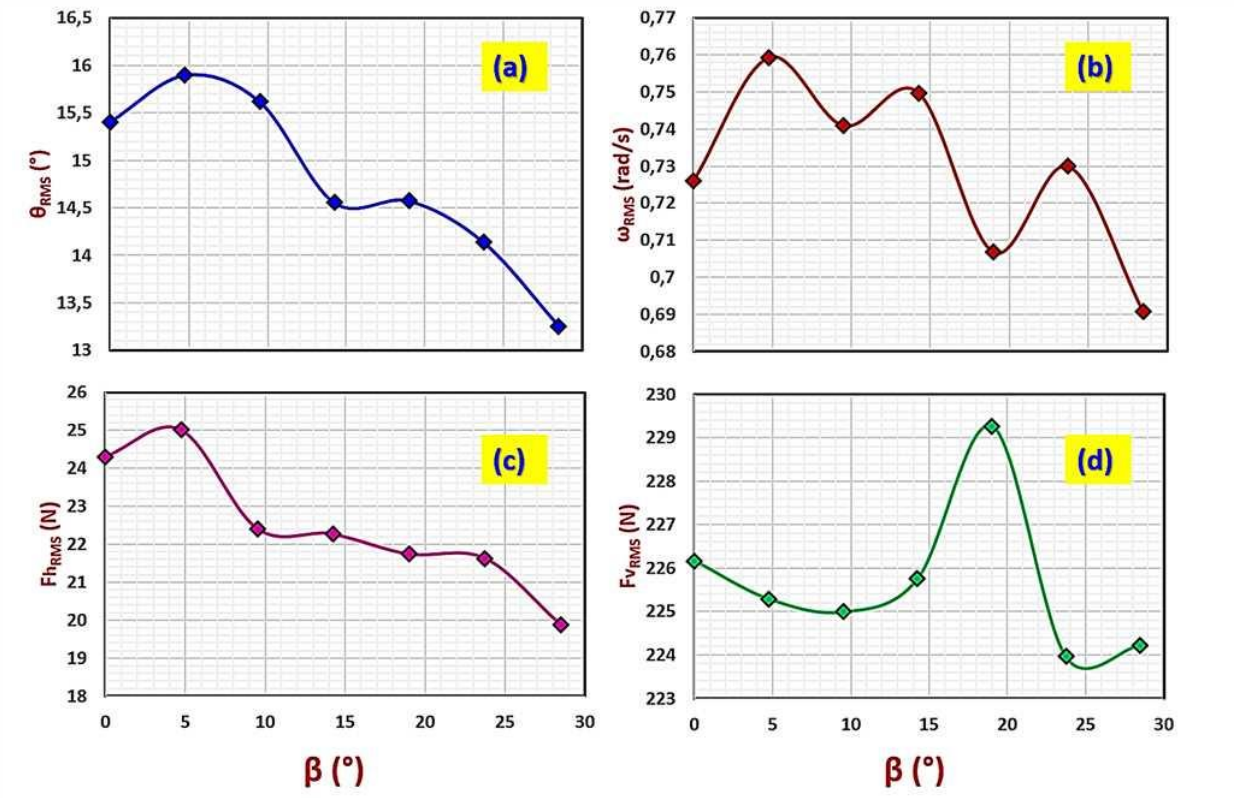

The RMS value of the angular velocity oscillates considerably as a function of the bottom slope, as presented in Figure 6b, indicating that an increase in this variable is associated with a strong influence on the oscillatory behavior of the structure. Comparing the maximum RMS value of the angular velocity (observed at a slope of 5°) with the minimum value observed for this variable (at 28.49°), it can be concluded that an increase in the bottom slope can cause a variation of up to 9,00% in the angular velocity of the OWSC.

The RMS value of the horizontal force (Figure 6c) presents a behavior similar to the maximum and minimum values observed for this same variable (as presented in Figure 5c) as a function of the slope bottom slope. Thus, the horizontal force tends to increase first for slopes of up to 5°, decreasing on slopes greater than this. The RMS value of the vertical force (Figure 6d) demonstrates a small increase (around 1,40%) on slopes between 15° and 20°, an interval that corresponds to the minimum RMS value observed for the angular velocity, representing a range of unfavorable slopes for the hydrodynamics of the converter.

Figure 7.- Variation of the RMS value of the excitation torque and the average captured power, depending on the bottom slope.

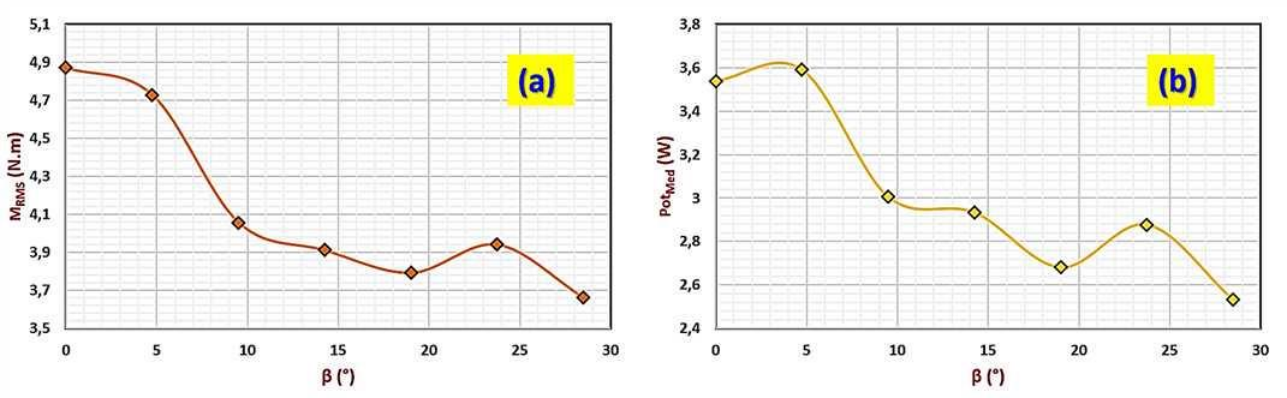

By analyzing the graphs shown in Figures 7a and 7b, a close similarity can be observed between the curves of the RMS values of the excitation torque and the average captured power, indicating that the excitation torque is a very important variable on the flap hydrodynamics. On the other hand, it can be concluded that the increase of 1,50% experienced in the average captured power for a slope of 5° is due to the influence of the angular velocity (which presents the same behavior, observed in Figure 6b). In general, comparing the first and the last case, it is possible to observe decreases close to 28% in the excitation torque and in the converter average captured power, leading to the conclusion that the increase in the bottom slope causes unfavorable flow characteristics to the hydrodynamics of the flap, resulting in low efficiency of the electric energy generated by the system.

4 CONCLUSIONS

In the present study, the free and open-source code OpenFOAM was applied to evaluate the influence of the ocean bottom slope on hydrodynamics and energy generation by the Oscillating Wave Surge Converter system. Seeking a sufficiently accurate and adequate modeling, with satisfactory representation of the associated turbulent phenomena, it was chosen to use the numerical methodology based on Large Eddy Simulation (LES) through the application of a two-dimensional WALE model.

The results showed that the increase on the bottom slope significantly influences the hydrodynamic parameters of the converter. Slopes between 0° and 5° are favorable for energy generation, as slopes in this range can cause an increase in the angular velocity experienced by the flap, resulting in an increase in the average captured power. However, for slopes greater than 5º, the hydrodynamic variables tend to decrease their magnitudes, resulting on a significant drop in the energy produced by the system.

The lowest captured power values occur on slopes greater than 15º, due to the increase in vertical force, decrease in horizontal force, angular displacement and angular velocity. Therefore, it is possible to conclude that the ideal region to install the OWSC's is the one with a mild slope. However, when

installation is necessary in regions with steeper slopes, one should choose to install the OWSC's partially submerged on floating platforms, thus ensuring that their base is far from the bottom, reducing the influence of the bottom slope on the hydrodynamics of the converter.

ACKNOWLEDGMENTS

We thank CNPq for the resources invested during the research and the UFRGS university for the structure and support in the development of the numerical simulations.

REFERENCES

Bourgoin, A.C., Guillou, S.S., Thiébot, J., Ata, R. (2020). "Turbulence characterization at a tidal energy site using large-eddy simulations: case of the Alderney Race". *Philosophical Transactions of the Royal Society A*, 378(2178), 20190499.

Brito, M., Canelas, R. B., García-Feal, O., Domínguez, J. M., Crespo, A. J. C., Ferreira, R. M. L., ... Teixeira, L. (2020). " A numerical tool for modelling oscillating wave surge converter with nonlinear mechanical constraints ". *Renewable Energy*, 146, 2024-2043.

Curto, D.; Franzitta, V.; Guercio, A. (2021). " Sea wave energy. A review of the current technologies and perspectives ". Energies, 14 (20), 6604.

Esteban, G.A., Aristondo, A., Izquierdo, U., Blanco, J. M., Pérez-Morán, G. (2022). " Experimental analysis and numerical simulation of wave overtopping on a fixed vertical cylinder under regular waves ". *Coastal Engineering*, 173, 104097.

Fuhrmeister, G. V. (2020). "Validação de um modelo 2D para a simulação numérica em grandes escalas de um conversor de ondas do tipo OWSC". *Anais do III Encontro Sul Brasileiro de Engenharia Ambiental e Sanitária (ESBEA)*, Caxias do Sul, Brasil.

Gallutia, D., Fard, M.T., Soto, M. G., He, J. (2022). " Recent advances in wave energy conversion systems: From wave theory to devices and control strategies ". *Ocean Engineering*, 252, 111105.

Ghasemipour, N., Izanlou, P., Jahangir, M. H. (2022). " Feasibility study on utilizing oscillating wave surge converters (OWSCs) in nearshore regions, case study: Along the southeastern coast of Iran in Oman sea ". *Journal of Cleaner Production*, 133090.

Higuera, P. (2016). *OLAFOAM Reference Manual*. Spain, Cantábria.

Jin, S., Zheng, S., Greaves, D. (2022). "On the scalability of wave energy converters". *Ocean Engineering*, 243, 110212.

Kelly, M.; Tom, N.; Yu, Y.H.; Wright, A.; Lawson, M. (2021). "Annual performance of the second-generation variable-geometry oscillating surge wave energy converter". *Renewable Energy*, 177, 242-258.

National Renewable Energy Laboratory. (2021). "*Shoring Up Wave Energy's Bottom Line Through Variable-Geometry WEC Designs*". Available in: <https://www.nrel.gov/news/program/2021/shoring-up-wave-energys-bottom-line-through-variable-geometry-wec-designs.html>.

Langlee Wave Power. (2013). *"Langlee 132kW Robusto"*. Available in: <http://www.langleewp.com/>.

Launchbury, D. R. (2016). *Unsteady turbulent flow modelling and applications*. Springer.

Liu, Y., Cho, Y.H., Mizutani, N., Nakamura, T. (2022). " Study on the resonant behaviors of a bottom-hinged oscillating wave surge converter ". *Journal of Marine Science and Engineering*, 10(1), 2.

Liu, Z., Wang, Y., Hua, X. (2021). "Proposal of a novel analytical wake model and array optimization of oscillating wave surge converter using differential evolution algorithm". *Ocean Engineering*, 219, 108380.

Wei, Y., Rafiee, A., Henry, A., Dias, F. (2015). "Wave interaction with an oscillating wave surge converter, Part I: Viscous effects". *Ocean Engineering*, 104, 185-203.

Wei, Y., Abadie, T., Henry, A., Dias, F. (2016). "Wave interaction with an oscillating wave surge converter. Part II: Slamming". *Ocean Engineering*, 113, 319-334.

Windt, C., Davidson, J., Ringwood, J. V. (2018). "High-fidelity numerical modelling of ocean wave energy systems: A review of computational fluid dynamics-based numerical wave tanks ". *Renewable and Sustainable Energy Reviews*, 93, 610-630.